Chinese Journal of Polymer Science Vol. 34, No. 11, (2016), 1339–1353

Chinese Journal of Polymer Science

An Efficient Halogen-free Flame Retardant for Polyethylene: Piperazine-modified Ammonium Polyphosphates with Different Structures*

Shi-fu Liao, Cong Deng**, Sheng-chao Huang, Jing-yu Cao and Yu-zhong Wang**

Center for Degradable and Flame-Retardant Polymeric Materials, College of Chemistry, State Key Laboratory of Polymer Materials Engineering, National Engineering Laboratory of Eco-Friendly Polymeric Materials (Sichuan); Analytical and Testing Center, Sichuan University, Chengdu 610064, China

Abstract In this study, piperazine-modified ammonium polyphosphates (PA-APPs) with hierarchical structure were synthesized through ion exchange reaction. ^{1}H nuclear magnetic resonance (^{1}H-NMR), Fourier transform infrared spectra (FTIR), elemental analysis (EA), and inductively coupled plasma atomic emission spectroscopy (ICP-AES) confirmed that the PA-APPs with different structures were prepared successfully. Then these flame retardants were used alone as mono-component intumescent flame retardant for low-density polyethylene (LDPE). Combustion tests demonstrated that the flame-retardant efficiency of PA-APP containing about 7 wt% carbon (PA-APP$_7$) was significantly higher than that of the other PA-APPs with more or less carbon. The flame-retarded LDPE system with 30 wt% PA-APP$_7$ passed the UL-94 V-0 rating, and had the oxygen index (LOI) of 33.0%. Thermal analysis illustrated that the thermal decomposition behavior of PA-APP changed with incorporating different contents of PA. For all these PA-APPs, PA-APP$_7$ showed higher thermal stability than the other PA-APP flame retardants. All the experimental results proved that PA-APP$_7$ could reach the balance of an acid source, a blowing source, and a charring source as a mono-component intumescent flame retardant for LDPE. Further, it led to the formation of a compact intumescent char layer containing the structures of rich P—O—P, P—N—C, C=C, *etc*. during burning which in turn resulted in the excellent flame-retardant efficiency of PA-APP$_7$.

Keywords: Ammonium polyphosphate; Piperazine; Flame retardant; Polyethylene.

INTRODUCTION

Low-density polyethylene (LDPE), with outstanding characteristics of low toxicity, excellent electric insulation, good chemical resistance, high mechanical durability, and ease of processing and molding, has been widely used in many fields[1–4]. For the sake of public safety, the majority of LDPE products, especially for wires and cables, have to pass regulatory flame-retardant tests. Unfortunately, LDPE has high flammability[4–6], such as low limiting oxygen index (LOI), melt dripping, easy fire spreading, and so on, which restricts its application in flame-retarded materials. Therefore, flame-retardant modification for LDPE is necessary to meet the market demand.

Traditional halogenated compounds are effective to improve the flame retardancy of LDPE, especially in the combination with antimony trioxide[7, 8]. However, these halogen-containing flame retardants are being phased out because of their environmental hazard. At present, more attention has been focused on exploring

* This work was financially supported by the National Natural Science Foundation of China (No. 51421061) and the Program for Changjiang Scholars and Innovative Research Team in University (No. IRT1026).
** Corresponding authors: Cong Deng (邓聪), E-mail: dengcong@scu.edu.cn
Yu-zhong Wang (王玉忠), E-mail: yzwang@scu.edu.cn
Received May 25, 2016; Revised June 21, 2016; Accepted June 28, 2016
doi: 10.1007/s10118-016-1855-8

novel halogen-free flame retardants, such as metal hydroxide[9–12], metal borates[13, 14], organic phosphorus-based flame retardants[15–17], nitrogen-based flame retardants (melamine *etc*.)[18–20], intumescent flame retardants (IFRs)[21–24], *etc*. For metal hydroxide-filled PE, the loading of flame retardant is quite high to achieve the good flame retardancy of PE. Generally, its content is higher than 50 wt%, which lead to the serious deterioration of mechanical properties of the PE. Metal borates are not very efficient when they were used alone to flame retard PE, which are usually applied in combination with halogenated compounds to improve their flame-retardant efficiency, so their application are limited at present. Phosphorus-based flame retardants, including phosphates, phosphonates, phosphinates, phosphine oxides and red phosphorus, can also be used to flame retard PE. However, these flame retardant are particularly effective for polymers containing oxygen (polyesters, polyamides, cellulose, *etc*.), so it is not a good choice to flame retard PE. Nitrogen-based flame retardants, such as melamine, triazine, and melamine polyphosphate *etc*., were also used to flame retard PE, in which the most effective one should be melamine polyphosphate. However, the UL-94 V-0 could not be achieved even when its loading was higher than 30 wt%. For these halogen-free flame retardants, IFRs have been proved to be very effective to flame retard polyolefin[25–27]. Nie *et al*.[28] studied the effect of IFR on the flame retardancy of LDPE, and found that LDPE/IFR composite could pass the UL-94 V-0 rating, and had a LOI of 29.0% at the loading of 30 wt% flame retardant. Camino *et al*.[29, 30] discussed the flame retardant mechanism of IFR in detail.

Generally, an IFR mainly contains three components, which are an acid source, a blowing agent, and a charring agent, respectively. APP, as a combination of an acid source and a blowing agent, has low efficiency to flame retard polyolefin when it is used alone, while it is very efficient to flame retard polyolefin together with a charring agent. However, charring agents have two disadvantages in current application. The first one is that their preparation processes are very complicated, for example, Li and Xu[31], reported that the preparation of the piperazine derivatives used as charring agents need three complicated steps; the second one is that the raw materials or products to prepare the charring agent are harmful to the environment, for instance[32], the deleterious cyanuric chloride, phosphorus oxychloride, and trichloromethane are usually used to prepare charring agents. Therefore, it should be an ideal way to create a mono-component intumescent flame retardant to achieve the flame retardation of polyolefin. Since APP gathers the characteristics of the acid source and blowing agent, it should be a good choice to fabricate a mono-component IFR based on it.

In our previous research[33–35], several mono-component IFRs were prepared *via* cation exchange reaction, in which PA-APP was confirmed to be efficient to flame retard polypropylene (PP). However, the PA-APPs prepared under different conditions have various structures. For PA-APP, the contents of phosphorus, nitrogen and carbon represent the acid source, blowing source and charring source respectively. Obviously, the change of the structure of PA-APPs indicates that the components of the three sources for these flame retardants are different, which can directly affect their flame-retardant efficiency. So far, there is no comprehensive insight into the hierarchical structure of PA-APP, so the effect of the difference for structures of PA-APP on the flame retardancy of polymer is still not well understood. To clearly know about it, it is very meaningful to have a deep study on the hierarchical structure of PA-APP. Moreover, as a vital factor, the balance feature of an acid source, a charring source, and a blowing source for PA-APP is also not confirmed in previous work, so the current work on the hierarchical structure of PA-APP is very important and necessary.

In current work, a series of chemically-modified PA-APPs with different structures were synthesized, and an insight into the structure of these PA-APPs was carried out, meanwhile, their corresponding flame-retardant efficiency for LDPE was also investigated by LOI, UL-94, and CC tests. Then, the relationship between the flame-retardant efficiency of PA-APPs and their structures was established. Moreover, the PA-APP with the balance of an acid source, a blowing source, and a charring source was confirmed in the present work. In addition, its flame-retardant mechanism was also discussed with the aid of FTIR, thermogravimetric analysis (TGA), scanning electronic microscopy (SEM), and X-ray photoelectron spectroscopy (XPS).

EXPERIMENTAL

Materials

LDPE (2426H) was purchased from Petro China Lanzhou Petrochemical Co., Ltd. (Lanzhou, China). Commercial APP (form II, the degree of polymerization ≈ 1000) was supplied by Taifeng New-Type Flame Retardants Co., Ltd. (Shifang, China). Piperazine (AR) and ethanol (AR) were purchased from Tianjin Kemiou Chemical Reagent Co., Ltd. (Tianjin, China) and Kelong Chemical Reagent Co., Ltd. (Sichuan, China), respectively.

Preparation of PA-APP Flame Retardants

Firstly, ethanol (600 mL) and water (25, 30, 35, 40, 45, 50 and 55 mL, respectively) were poured into a 2 L three-neck glass flask equipped with a stirrer and a reflux condenser under a nitrogen atmosphere. After half an hour, PA (86 g, 1 mol) was added into the flask with stirring. After the PA was dissolved completely, 100 g of APP was added in the flask. The mixture was heated up to 90 °C for 4 h, and accompanied by stirring. After the completion of reaction, the mixture was cooled down to room temperature, and then filtered. The obtained white solid was washed with ethanol, and then dried to a constant weight at 80 °C in a vacuum oven. Finally, PA-APP flame retardants with hierarchical structure were obtained, and denoted as PA-APP_2, PA-APP_4, PA-APP_7, PA-APP_{11}, PA-APP_{14}, PA-APP_{17}, and PA-APP_{22}, respectively, corresponding to their carbon contents of about 2 wt%, 4 wt%, 7 wt%, 11 wt%, 14 wt%, 17 wt% and 22 wt%.

Samples Preparation for Different Tests

Samples preparation for burning tests

In our work, APP or PA-APPs was blended with LDPE through extruding. The detailed process is as follows. Both LDPE and APP (or PA-APP) were mixed firstly, then the LDPE containing different weight ratios of APP or PA-APP were extruded *via* a twin-screw extruder (CTE 20, Kebeilong Keya Nanjing Machinery Co., Ltd, Nanjing, China) under the rotation speed of 150 r/min at the following temperature protocol from the feed zone to the die: 160, 165, 170, 165, 160 and 150 °C. Next, the obtained pellets were hot-pressed into sheets with the thickness of 3.2 mm through plate vulcanizing machine (Qingdao Yadong Rubber Machinery Co. Ltd. China) to measure the flame retardancy of LDPE, LDPE/APP and LDPE/PA-APP systems.

Residues for FTIR and XPS tests

LDPE composites were heated to the corresponding temperature at a heating rate of 10 K/min under a nitrogen atmosphere in TG and maintained for 10 min at each temperature, and then these residues for FTIR and XPS tests were obtained. Here, the choice of these temperatures is dependent on TG results of APP and PA-APP.

Characterization

Fourier transform infrared spectra (FTIR) were recorded by a Nicolet FTIR 170SX spectrometer (Nicolet, America) using the KBr disk. APP or PA-APPs (1 mg) and KBr (100 mg) were mixed in agate mortar, then compressed into the sheets with 1 mm thickness. The wave number range was set from 4000 cm^{-1} to 500 cm^{-1}.

The ^{1}H-NMR spectra were recorded on a Bruker AV II-400 MHz spectrometer (Bruker, Switzerland) by using D_2O as a solvent.

The contents of carbon (C), nitrogen (N) and hydrogen (H) in APP and PA-APP were measured by elemental analysis (EA) on CARLO ERBA1106 instrument (CarloErba, Italy). The contents of phosphorus (P) in APP and PA-APP were determined by inductively coupled plasma atomic emission spectroscopy (ICP-AES, IRIS Advantage, TJA solution). The tested samples for APP and PA-APPs were prepared as follows. The 5 mg of powder was dissolved into 10 mL of concentrated hydrochloric acid in a 100 mL flask, and kept for 48 h; then a certain amount of distilled water was added into the flask to a constant volume (100 mL).

The TGA was carried out by a thermogravimetric analyzer instrument (TG209 F1, NETZSCH, Germany) at a heating rate of 10 K/min under the nitrogen flow of 50 mL/min in the temperature range from 40 °C to 700 °C.

The SEM observation was performed by a FEI scanning electron microscope (Inspect F, FEI, USA) at an

accelerating voltage of 10 kV to study the surface of char residues obtained from CC tests. All specimens were coated with a conductive layer before being examined.

Tensile test was carried out in accordance with the procedures in GB/T 1040.1-2006 at a crosshead speed of 50 mm/min. The Izod impact test was performed in accordance with the procedures in GB/T 1843-2008, and the depth of nick is 2 mm.

The LOI value was measured by a limiting oxygen index instrument (HC-2C, Jiangning Analytical Instrument Factory, China) using the sheets with the dimension of 130 mm × 6.5 mm × 3.2 mm according to ASTM D2863-97.

The UL-94 vertical burning level was tested on a vertical burning test instrument (CZF-2, Jiangning Analytical Instrument Factory, China) according to ASTM D3801. The dimension of samples is 130 mm × 13 mm × 3.2 mm.

The flammability of samples was measured by a CC device (Fire Testing Technology, East Grinstead, UK). The samples with the dimension of 100 mm × 100 mm × 3 mm were wrapped in aluminum foil and exposed to a radiant cone at a heat flux of 50 kW/m^2.

The XPS test was performed by a XSAM80 (Kratos Co, UK), using Al Kα excitation radiation ($h\nu$-1486.6 eV).

RESULTS AND DISCUSSION

Characterization of PA-APP Flame Retardants with Hierarchical Structure

FTIR and ^{1}H-NMR results

FTIR spectra of APP and PA-APP flame retardants are shown in Fig. 1. For PA-APPs, all typical peaks of APP still exist. The peaks observed in the 3400–3030 cm^{-1} region are ascribed to the asymmetry stretching vibration bond of NH_4^+[33], indicating that part of NH_4^+ was still kept in PA-APPs, and did not engage in the reaction between PA and APP. Some new absorption peaks appeared in PA-APPs compared with those of APP. These new stretching vibration absorption peaks of $-NH_2^+$ were found at 2498 cm^{-1}, indicating that PA might be incorporated into APP successfully. The new peaks located at 3448 and 1562 cm^{-1} are attributed to the stretching and flexural vibration of N—H respectively which always exist in PA-APPs, implying that the N—H in PA did not completely involve in the reaction between PA and APP. The peak appears at about 2818 cm^{-1} for the PA-APPs flame retardants, which is assigned to the symmetrical stretching vibration of $-CH_2-$[34]. When the amount of PA reacted with APP is little, the peak corresponding to $-CH_2-$ at 2818 cm^{-1} is very weak. With increasing the amount of PA in APP, the peak at 2818 cm^{-1} becomes more obvious. In addition, the peaks corresponding —N—H and $-NH_2^+$ have the same changing tendency, suggesting that more PA reacted with APP with increasing the water content in the solvent. Here, it should be noted that quantitative analysis for the FTIR result was not carried out. However, the mass of all FTIR samples are the same, including 1 mg of APP (or PA-APPs) and 100 mg of KBr, and the thickness of these samples are 1 mm. In addition, the experimental conditions are the same for all these samples, so the fact that these vibration peaks of both $-NH_2^+$ and N—H become higher might indicate that more PA reacted with APP. Of course, the results must be further confirmed by the following measurements.

To confirm the structure and the purity of the PA-APP flame retardants, the ^{1}H-NMR test was performed, and the result is presented in Fig. 2. For APP, only a peak appeared at about δ = 4.80, which is ascribed to a small residual concentration of H_2O or HOD in D_2O solvent[36]. A new peak at about δ = 3.49 corresponding to the $-CH_2-$ protons in ($-CH_2-NH_2^+$) appeared for PA-APP$_2$, demonstrating that PA-APP was synthesized successfully. From Figs. 2(b) to 2(h), the chemical shifts corresponding to the $-CH_2-$ protons are δ = 3.49, 3.48, 3.45, 3.38, 3.32, 3.20 and 3.15, respectively. Obviously, the chemical shift corresponding the $-CH_2-$ protons moved to a low shift gradually with the increase of the content of C. Here, it should be noted that the corresponding chemical structure of PA-APP may evolve according to the route shown in Scheme 1 with

increasing the C in PA-APP. The change in tendency for the structure of PA-APP is explained as follows. With the increase of the content of C, the decrease of electrostatic action near the H of $-CH_2-$ in PA-APP might result in a lower shielding effect for the H, so the chemical shift moved to low field with increasing the content of C in PA-APP. All the chemical shifts of PA-APPs are higher than $\delta = 2.71$ which corresponds to the $-CH_2-$ of neat PA[33], indicating that there was no piperazine left in these PA-APP flame retardants.

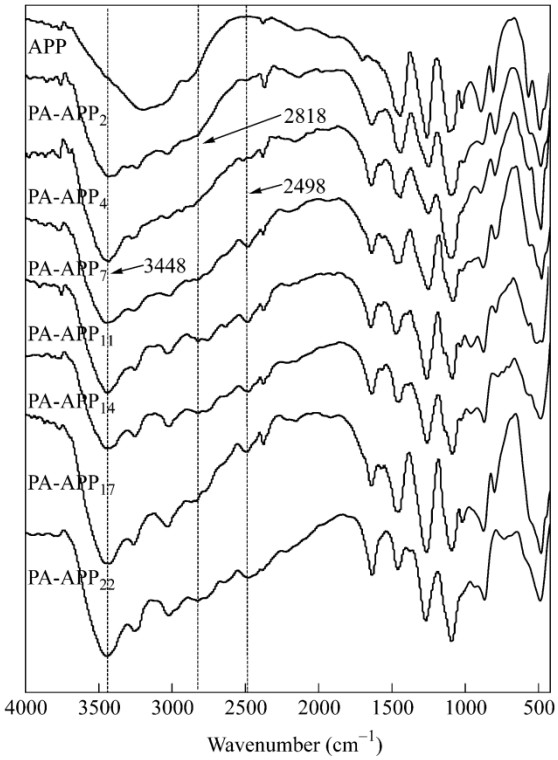

Fig. 1 FTIR spectra of series of PA-APP

Elemental analysis

Theoretically, there is no C in APP, therefore, the increase of C for PA-APP was used to confirm the successful preparation of PA-APP from the elemental viewpoint, and the difference of the contents of C for PA-APP flame retardants can be used to indicate various PA-APP. The EA was used to detect the element contents of carbon (C), nitrogen (N), and hydrogen (H) in PA-APP; while the ICP was used to measure the content of phosphorus (P) in PA-APP. The corresponding data are listed in Table 1. For the APP that we used in this work, its average polymerization degree is about 1000. Thus, its structure can be abbreviated to $(NH_4PO_3)_n$ ($n \approx 1000$). According to contents of C and P, the corresponding amount of PA and APP can be calculated, and the result is shown in Table 1. With the increase of the PA, the molar ratio between APP and PA decreased gradually, implying that the molar ratio of the charring source increased in this case. In addition, the H content of PA-APP also increased with the increase of the C. However, the N content of the PA-APP showed a little change, the main reason should be that both the incorporated N from PA and the released N accompanied by the production of ammonia reached a balance.

According to element analysis, FTIR and ^{1}H-NMR results, it can be confirmed that PA participated in the reaction with APP, and the chemically-modified PA-APPs with different structures were prepared successfully.

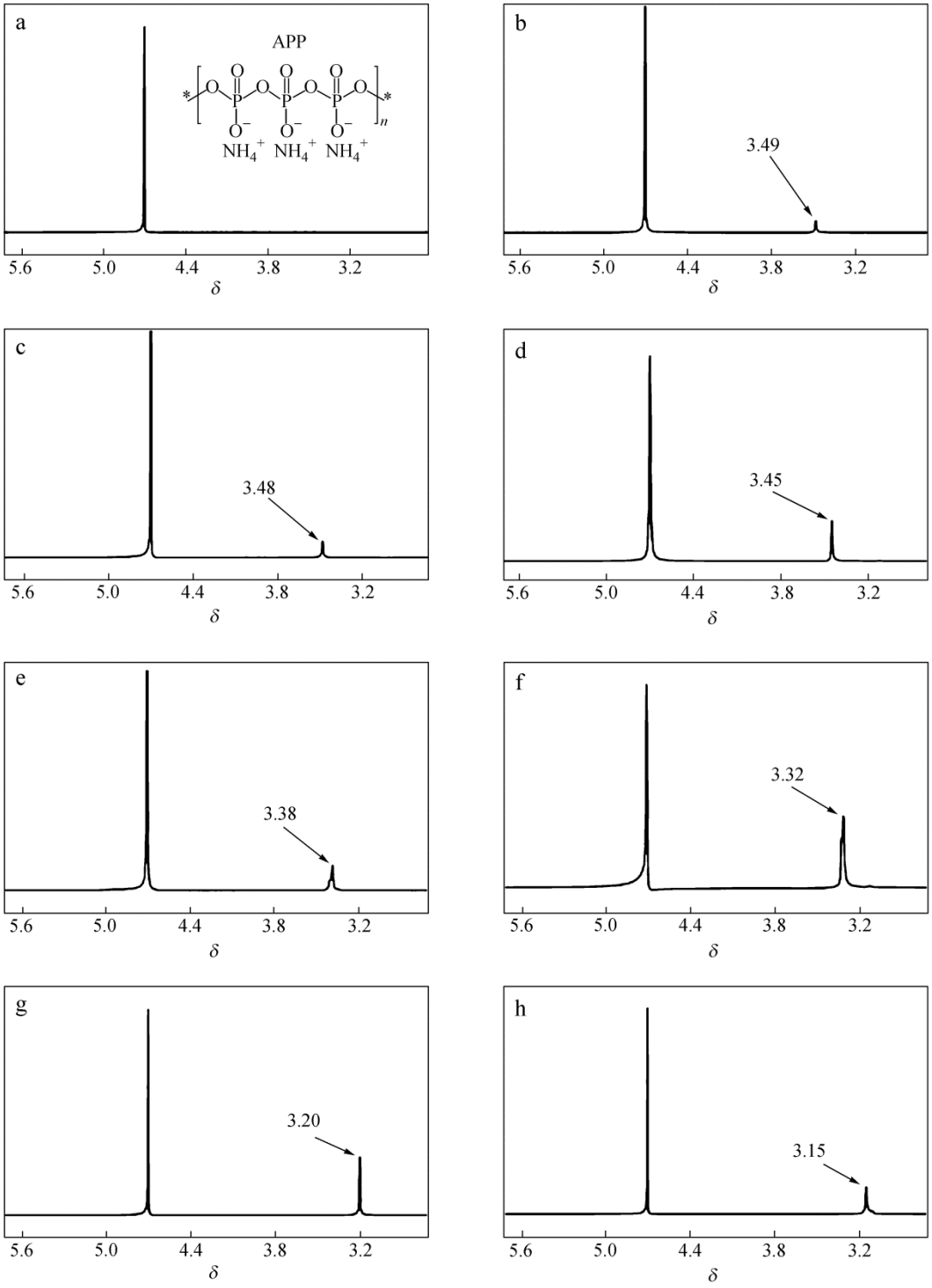

Fig. 2 ^{1}H-NMR spectra of APP and PA-APPs: (a) APP, (b) PA-APP$_2$, (c) PA-APP$_4$, (d) PA-APP$_7$, (e) PA-APP$_{11}$, (f) PA-APP$_{14}$, (g) PA-APP$_{17}$ and (h) PA-APP$_{22}$

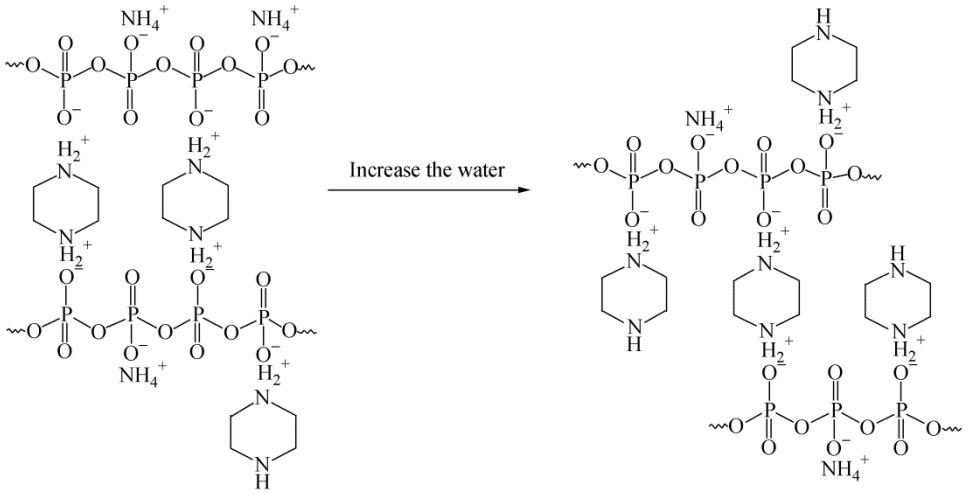

Scheme 1 Structural change of PA-APP with increasing PA content

Table 1. Elemental contents of C, H, N, and P in APP and PA-APP

Sample	C content (%)	H content (%)	N content (%)	P content (%)	P/C	APP/PA (molar ratio)
APP cal.	0	4.12	14.43	31.96	–	–
APP tested	0.01	4.17	14.44	31.15	–	–
PA-APP$_2$	2.42	4.31	14.49	31.02	12.82	19.85
PA-APP$_4$	4.15	4.42	14.31	30.38	7.32	11.33
PA-APP$_7$	7.04	4.80	15.96	29.34	4.17	6.45
PA-APP$_{11}$	11.21	5.43	12.26	27.22	2.43	3.76
PA-APP$_{14}$	14.13	5.92	12.75	26.09	1.85	2.86
PA-APP$_{17}$	17.23	6.26	12.89	24.74	1.44	2.22
PA-APP$_{22}$	22.58	7.70	13.76	22.13	0.98	1.52

"–" represents that there is no available data.

Flame Retardancy of LDPE/PA-APP Systems

To investigate the effect of the PA-APPs on the flame retardancy of LDPE, LOI and UL-94 tests were performed for neat LDPE and LDPE/PA-APP systems. The corresponding data are shown in Table 2. Both LOI and UL-94 results show that neat LPDE is a flammable polymer. When the loading of APP was 30 wt%, the LOI value reached 20.8%, higher than that of neat LDPE, but obvious dripping was observed for the APP system, which is the main reason for the fire spread in fire hazard. All LDPE/PA-APP systems got higher LOI than that of neat LDPE or LDPE/APP with equal amount of flame retardant. In UL-94 test, LDPE containing 30 wt% PA-APP$_2$, PA-APP$_{17}$ or PA-APP$_{22}$ had no rating, accompanied by dripping. Only LDPE containing 30 wt% PA-APP$_7$ or PA-APP$_{11}$ passed the V-0 rating, and no dripping was observed during burning. Here, it is found that the flame-retardant efficiency of PA-APPs was not linearly improved with increasing the PA in PA-APP, and the PA-APP$_7$ was the most effective to flame retard LDPE.

Due to the excellent flame-retardant efficiency of PA-APP$_7$, its effect on the flame retardancy of LDPE was further investigated, and the result is shown in Table 3. When the loading of PA-APP was 26 wt%, the LOI value of LDPE/ PA-APP$_7$ reached at 29.0%, and it could pass the UL-94 V-2 rating, accompanied by dripping during burning. At 28 wt% PA-APP, LDPE/PA-APP passed the UL-94 V-0 rating, and no dripping was observed. In addition, its LOI value was 31.5%, slightly lower than that of LDPE with 30 wt% PA-APP$_7$. In past research, Wu *et al*.[37] found that the LDPE with 30 wt% APP/PER (3/2) had the LOI of 26.5% and passed the UL-94 V-0 rating. Obviously, the flame-retardant efficiency of PA-APP$_7$ is higher than that of APP/PER. Compared with

the earlier report[6, 38], 30 wt% or more flame retardant is required to fulfill the UL-94 V-0 rating of LDPE. However, the loading of PA-APP as a mono-component intumescent flame retardant is lower than that of traditional highly-efficient compounded intumescent flame retardant.

Table 2. Flame reatardancy of neat LDPE and LDPE/PA-APP composites

Component			LOI (%)	UL-94 (3.2 mm)	
LDPE (wt%)	APP (wt%)	PA-APP (wt%)		Rating	Dripping
100	0	0	18.0	NR	Yes
70	30	0	20.8	NR	Yes
70	0	30/PA-APP$_2$	28.7	NR	Yes
70	0	30/PA-APP$_4$	30.7	V-2	Yes
70	0	30/PA-APP$_7$	33.0	V-0	No
70	0	30/PA-APP$_{11}$	31.5	V-0	No
70	0	30/PA-APP$_{14}$	29.0	V-2	Yes
70	0	30/PA-APP$_{17}$	27.6	NR	Yes
70	0	30/PA-APP$_{22}$	25.6	NR	Yes

Table 3. LOI and UL-94 results of LDPE/PA-APP$_7$

LDPE (wt%)	PA-APP$_7$ (wt%)	LOI (%)	UL-94 (3.2 mm)	
			Rating	Dripping
74	26	29.0	V-2	Yes
72	28	31.5	V-0	No
70	30	33.0	V-0	No

Mechanical Properties of LDPE, LDPE/APP and LDPE/PA-APP$_7$

Based on the excellent flame retardancy of PA-APP$_7$, the following work focuses on its effect on the flame retardancy and mechanical properties of LDPE, and its content in LDPE/PA-APP$_7$ is 30 wt%, denoted as LDPE/PA-APP$_7$. The mechanical properties of neat LDPE, LDPE/APP and LDPE/PA-APP$_7$ are listed in Table 4, including tensile strength, elongation at break, and impact strength. For LDPE/APP and LDPE/PA-APP$_7$, the tensile strength, elongation at break, and impact strength decreased significantly in the presence of 30 wt% flame retardant compared to the corresponding value of LDPE. At equal amount of flame retardant, both LDPE/APP and LDPE/PA-APP$_7$ have no apparent change in tensile strength, elongation at break, and impact strength.

Table 4. Mechanical properties of neat LDPE, LDPE/APP and LDPE/PA-APP$_7$

Sample	Tensile strength (MPa)	Elongation at break (%)	Impact strength (J/m)
LDPE	16.9 ± 0.5	780 ± 59	373.9 ± 13.1
LDPE/APP	8.7 ± 0.2	256 ± 25	187.5 ± 8.9
LDPE/PA-APP$_7$	8.6 ± 0.2	246 ± 22	190.1 ± 7.9

Combustible Behavior of LDPE/PA-APP$_7$ System

The CC test is an effective way to measure the flammable performance of flame-retarded polymer materials, so it was used to evaluate the flame-retardant efficiency of PA-APP$_7$. The CC data and curves of neat LDPE and its flame-retarded composites are presented in Table 5 and Fig. 3, respectively. The CC test showed that LDPE resin burned rapidly after the ignition, its peak value of heat release rate (PHRR) was 606.7 kW/m^2, and the total heat release (THR) value reached at 117.8 MJ/m^2 at the end of burning. When 30 wt% APP was incorporated into LDPE, the heat release rate (HRR) value was slightly reduced, and its PHRR was 483.2 kW/m^2, which was decreased by 20.4% compared to that of neat LDPE. In addition, the THR value was also reduced slightly to 100.5 MJ/m^2. Obviously, APP is not very efficient to flame retard LDPE when it is used alone. For LDPE/PA-APP$_7$ system, the HRR and THR values were decreased greatly to 173.1 kW/m^2 and 72.4 MJ/m^2 at 30 wt% PA-APP$_7$, respectively. Compared with the corresponding value of LDPE/APP, the PHRR and THR values of the LDPE/PA-APP$_7$ were reduced by 64.2% and 28.0%, respectively.

Table 5. CC data of neat LDPE, LDPE/APP and LDPE/PA-APP$_7$

Sample	LDPE	LDPE/APP	LDPE/PA-APP7
TTI (s)	45	24	25
PHRR (kW/m^2)	606.7	483.2	173.1
Time to PHRR (s)	195	110	130
THR (MJ/m^2)	117.8	100.5	72.4
Peak SPR (m^2/s)	0.068	0.057	0.021
TSP (m^2)	12.3	11.8	6.3
Residue (%)	0.01	24.74	36.82
Average MLR (g/s)	0.073	0.050	0.022

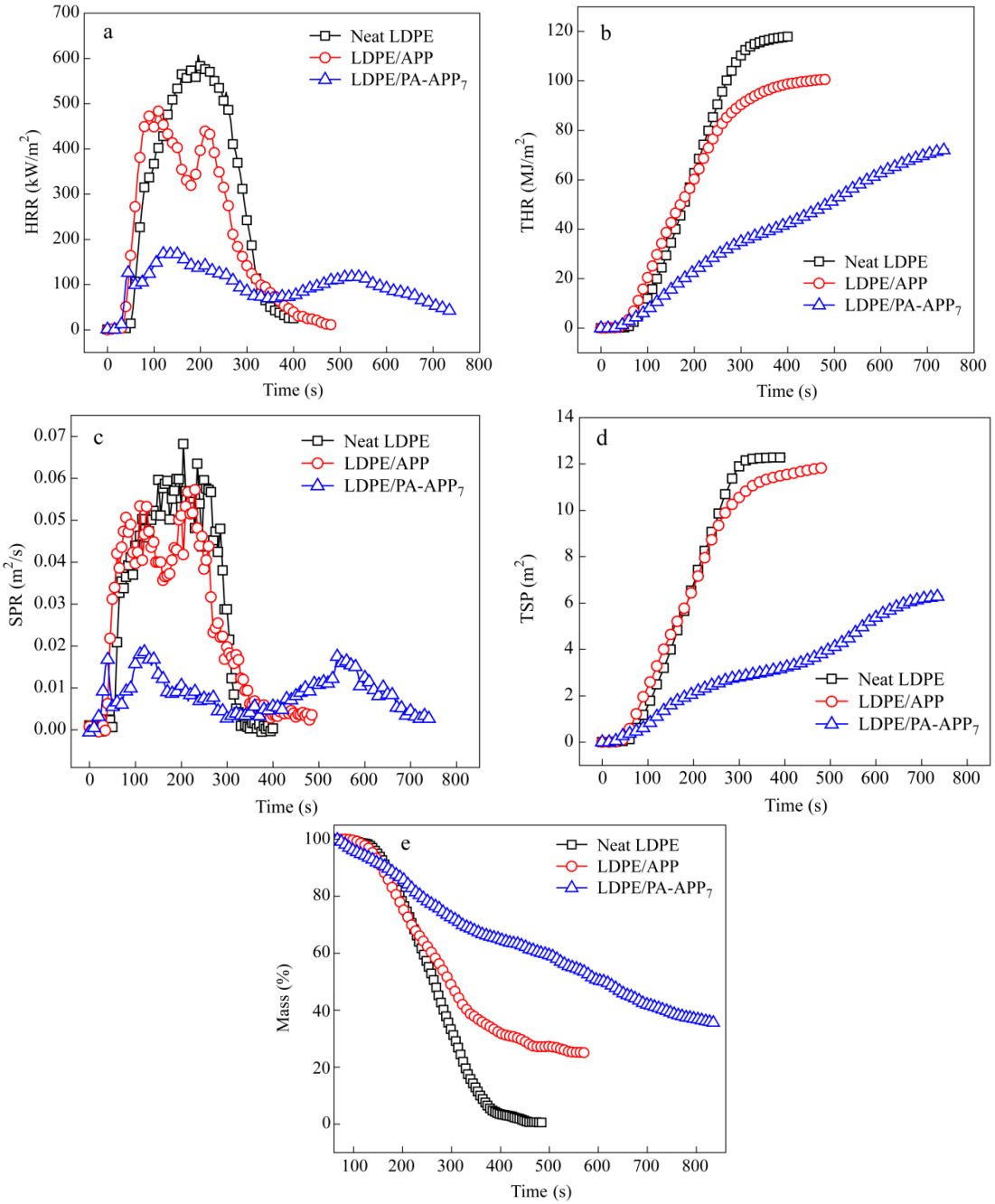

Fig. 3 (a) HRR, (b) THR, (c) SPR, (d) TSP and (e) ML curves of neat LDPE, LDPE/APP and LDPE/PA-APP$_7$

Similar to the HRR and THR curves, both the smoke production rate (SPR) and total smoke production (TSP) curves of flame-retarded LDPE composites present lower smoke release than that of neat LDPE in the presence of flame retardant. APP used alone could slightly decrease the peak of SPR and TSP value, which were decreased to 0.057 m^2/s and 11.8 m^2, respectively. With the incorporation of PA-APP_7, TSP and the peak of SPR were reduced to 6.3 m^2 and 0.021 m^2/s, respectively, which were correspondingly decreased by 69.1% and 48.5% compared with the two values of LDPE/APP system.

Mass lose (ML) curves are shown in Fig. 3(e). LDPE burned almost completely, and only 0.01 wt% residue was left at the end. For LDPE/APP and LDPE/PA-APP_7, their residues were 24.74% and 36.82%, respectively. For the average MLR, APP had a little effect on LDPE, which was decreased to 0.050 g/s from 0.073 g/s of neat LDPE. However, the MLR value of LDPE/PA-APP_7 composite decreased remarkably, and it was reduced to 0.022 g/s, which was decreased by 69.9% compared with that of LDPE/APP.

The digital photos of residues obtained after CC test for neat LDPE, LDPE/APP, and LDPE/PA-APP_7 are shown in Fig. 4. Neat LDPE burned almost completely. For LDPE/APP system, a residual char layer was observed after burning, which is not intumescent, and some obvious holes and cracks were formed in the char layer, as shown in Figs. 4(b) and 4(b_1). Generally, the poor char layer cannot inhibit the burning of polymer. For LDPE/PA-APP_7 composite, a thick, intumescent, and continuous char layer was formed during burning. Generally, the compact char layer on the surface of LDPE composite can prevent the heat and mass transfer between gas and condensed phase, and can also protect the underlying materials from further burning. So the formation of compact intumescent char layer should be an important factor to achieve the much better flame retardancy of LDPE/PA-APP_7 than that of LDPE/APP under equal amount of flame retardant.

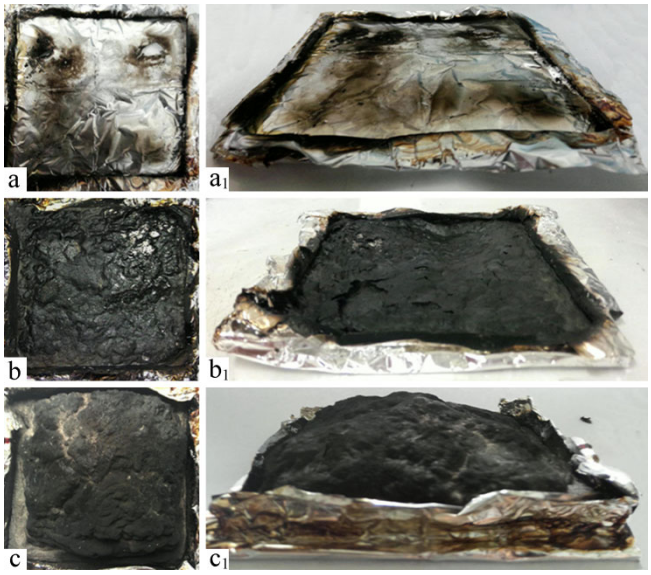

Fig. 4 Digital photographs for residues of (a, a_1) neat LDPE, (b, b_1) LDPE/APP, and (c, c_1) LDPE/PA-APP_7 after CC test

To further investigate the char layer of LDPE/PA-APP_7, its SEM images were recorded and are shown in Fig. 5. SEM results show that a three-dimensional network was formed in the outer layer of the residue of LDPE/PA-APP_7 after burning, and a compact char residue was deposited in the inner layer, both of which led to the formation of an compact char layer after CC test for LDPE/PA-APP_7.

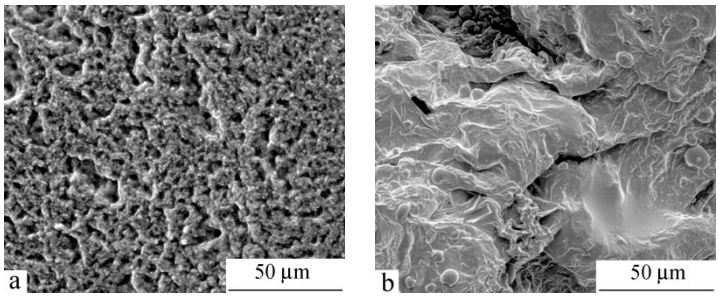

Fig. 5 SEM micrographs for (a) out and (b) inner layers of the residue of LDPE/PA-APP$_7$

Thermal Decomposing Behaviors of PA-APPs with Hierarchical Structure

To understand the reason for the difference of flame-retardant efficiency of PA-APPs with hierarchical structure, their thermal decomposing behaviors were analyzed firstly. TGA data and curves of PA-APP and APP under N_2 and air atmospheres are presented in Table 6 and Fig. 6, respectively. Under N_2 atmosphere, there are two drastic decomposing processes for APP. The first step is in the range from 200 °C to 450 °C, in which the weight loss should be attributed to the elimination of NH_3 and H_2O during the thermal decomposing process of polyphosphate[39]. The second step is from 480 °C to 600 °C. Here, the weight loss is attributed to the release of phosphoric acid, polyphosphoric acid, and metaphosphoric acid with the decomposition of APP[39]. Figure 6 indicates that each PA-APP flame retardant has a more complex thermal decomposing process than APP, which is consistent with the result presented in a previous paper[34]. Figure 6(a) shows that ML processes of PA-APP$_2$, PA-APP$_4$, or PA-APP$_7$ is similar with that of APP before 500 °C; while ML processes of PA-APP$_{11}$, PA-APP$_{14}$, PA-APP$_{17}$ or PA-APP$_{22}$ are different from that of APP in the same temperature range, in which they began to lose mass at about 100 °C. At above 500 °C, the ML of PA-APP flame retardants with lower than 7 wt% of C is less than that of APP. The residues of PA-APP$_2$, PA-APP$_4$, and PA-APP$_7$ at 700 °C were 28.1 wt%, 30.2 wt%, and 35.2 wt%, respectively, higher than that of APP; while the residues of PA-APP with higher than 7 wt% of C are significantly lower than that of APP, as shown in Table 6. Obviously, 7 wt% of carbon in these flame retardants is a turning point for the thermal stability of PA-APPs. The residues of PA-APP containing lower content of carbon at 700 °C is higher than that of PA-APP with higher content of C, which should be due to the structural difference of PA-APPs. According to the discussion presented above, we know that the content of C, P and N represents the charring source, acid source and blowing source, respectively. When the content of C is low, the charring source is insufficient. In this case, the enough acid source may dehydrate the charring source into char[40], so the residues of PA-APP increased with increasing the content of C in the range of low content of C. When the content of C is very high, the corresponding PA-APP has superfluous charring source, but lack of acid source, so part of charring source cannot be dehydrated into char, and decomposed into gas phase products, resulting in lower residue. Experimental result demonstrates that the PA-APP$_7$ has higher residue in the investigated range, namely, the ratio of acid source, charring source and blowing source in PA-APP$_7$ is optimal in the investigated range.

Figures 6(c) and 6(d) show thermal decomposition curves of APP and PA-APPs under air atmosphere. There are two severe decomposing steps for the APP, PA-APP$_2$, PA-APP$_4$ and PA-APP$_7$. The obvious difference for them is that the second decomposing stage of chemically-modified APP is quite different from that of APP. Compared with that of APP, the second decomposition temperature of PA-APP$_2$, PA-APP$_4$ and PA-APP$_7$ increased gradually, which might be due to the formation of a stable and compact char at the first decomposition stage, which delayed the second decomposition process[33]. For the PA-APP$_{11}$, PA-APP$_{11}$, PA-APP$_{17}$, and PA-APP$_{22}$, the decomposition processes in the range of 185 °C to 500 °C are quite complex. In the first step, the thermal decomposing process of these PA-APPs is different from that of APP, showing less stability compared to that of APP, which might be ascribed to the lack of acid source, then the majority of charring source (PA slat) decomposed into gas phase products. However, the second decomposition stage is similar to that of APP, which should correspond to the release of phosphoric acid, polyphosphoric acid, and metaphosphoric acid during the decomposition of APP, which contributed to the formation of stable residue[39].

Table 6. TGA data of APP and PA-APP retardants

Sample		APP	PA-APP$_2$	PA-APP$_4$	PA-APP$_7$	PA-APP$_{11}$	PA-APP$_{14}$	PA-APP$_{17}$	PA-APP$_{22}$
Residue (wt%)	N_2	27.5	28.1	30.2	35.2	22.5	22.9	23.5	25.2
	Air	26.5	8.7	9.6	11.4	10.0	9.8	9.0	6.2

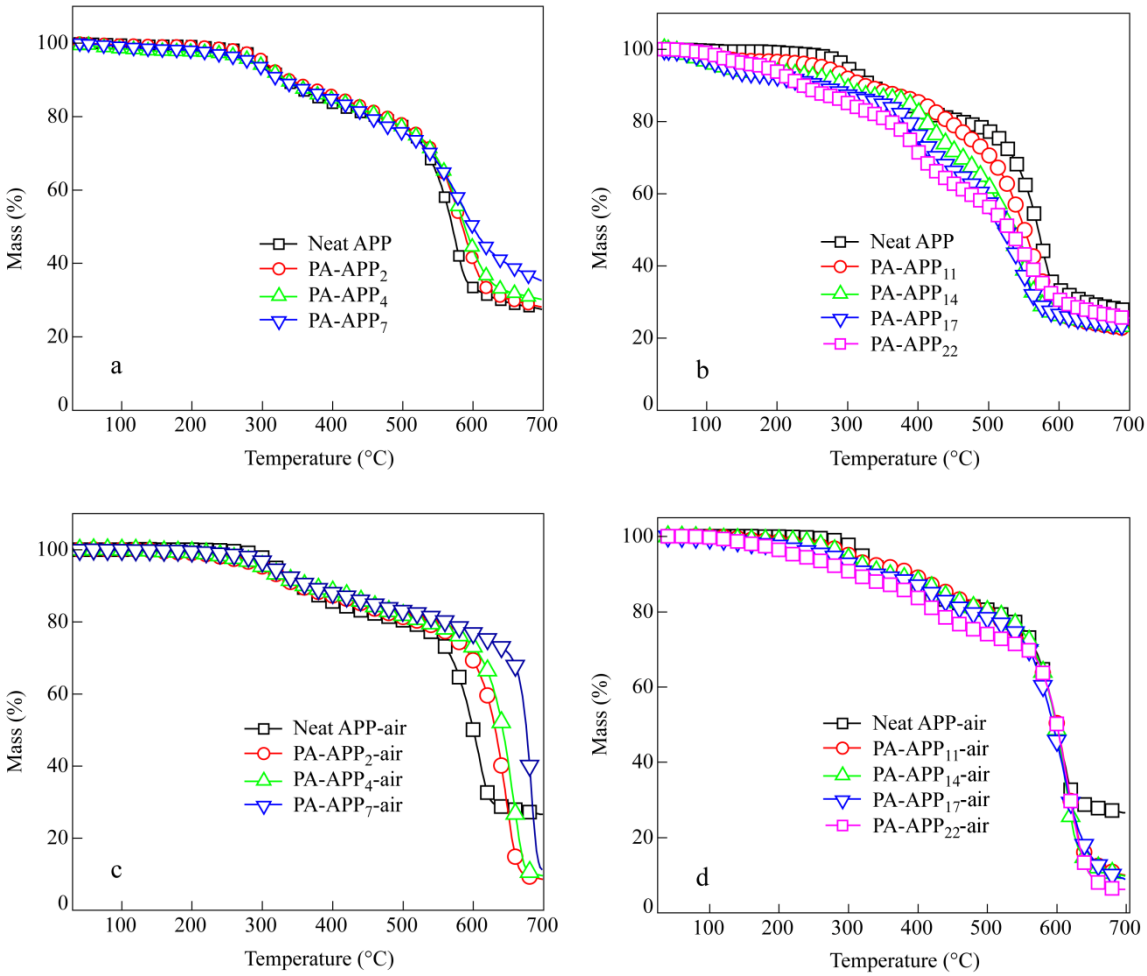

Fig. 6 TGA curves of APP and PA-APPs at a heating rate of 10 K/min under (a, b) N_2 and (c, d) air atmospheres

Flame-retardant Mechanism of PA-APP7 with the Balance of Three Sources

FTIR result of the residue of LDPE/PA-APP$_7$

FTIR spectra of the residues obtained at different temperatures for LDPE/PA-APP$_7$ are shown in Fig. 7. The peaks corresponding to the stretching vibration of NH_4^+ at 3030–3400 cm^{-1} decreased gradually with increasing the temperature, and almost disappeared at about 580 °C, indicating the release of large amounts of ammonia at less than 580 °C[41]. The P—O—P bond locating at 1260 and 850 cm^{-1} always existed during the whole decomposing process, illustrating that it had some contribution to the formation of a stable char layer. At 360 °C, the peaks corresponding to P—N—C structure appeared at 1086 and 723 cm^{-1}, and always existed until the temperature increased to 580 °C. In our previous study[33], it was well-established that the P—N—C rich char residue could facilitate the formation of a stable char layer at early stage, resulting in the promotion of the flame retardancy of polymer. The absorbing peak of —CH_2—CH_2— at 2822 cm^{-1} disappeared at about 480 °C,

suggesting that the structure was destroyed below 480 °C. The absorbing peak at 1636 cm^{-1} became wider with increasing the temperature, indicating the existence of the structures containing C=C in the residue[42], which could promote the charring of the residue. The results presented above demonstrated that the formation of the compact char layer should be due t o the formation of P—N—C, C=C, *etc*. structures during burning.

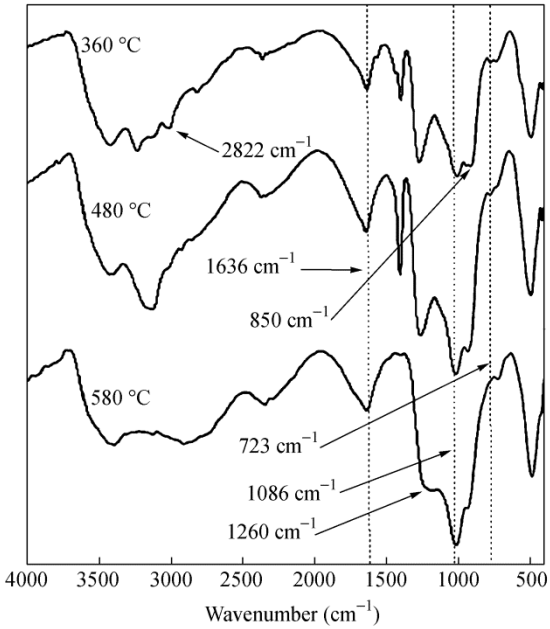

Fig. 7 FTIR spectra of the condensed products during the thermal decomposition of LDPE/PA-APP_7

XPS result of the residue of LDPE/PA-APP_7

In addition, XPS test was also used to study the elemental change of the condensed products of LDPE/APP and LDPE/PA-APP_7. The change of the elemental contents of C, N, O, and P are listed in Table 7. For the thermal decomposition of LDPE/APP, the contents of C and N decreased gradually, indicating the decomposition of LDPE and the release of the NH_3, respectively. The contents of P and O have a converse change tendency. With raising the temperature, both contents increased due to the formation of P—O—P or P—O—H structure in the condensed phase, accompanied by the decomposition of APP. For LDPE/PA-APP_7, the content of C increased to 75.6% at 480 °C, which is quite different from the change tendency of C in LDPE/APP system. Here, the increase of C should be due to the protection of a char layer formed before 480 °C. According to the FTIR analysis, the char layer might be composed of P—N—C, P—O—P, *etc*. structures. The content of N decreased greatly from 360 °C to 480 °C, which should be due to the release of NH_3 or gas containing —C=N. The contents of P and O decreased from 360 °C to 480 °C because of the deposition of C, further confirmed the flame-retardant contribution of PA-APP in this temperature range. Next, both contents increased due to the formation of P—O—C, P—N—C, *etc*. structures in the charring process.

Table 7. XPS data of the condensed products during the thermal decomposition for LDPE/APP and LDPE/PA-APP_7

Sample	*T* (°C)	C content (wt%)	N content (wt%)	P content (wt%)	O content (wt%)
LDPE/APP	360	58.2	4.7	13.3	23.8
	480	29.5	2.4	27.6	40.5
	580	26.1	1.8	26.9	45.2
LDPE/PA-APP_7	360	54.4	6.6	14.7	24.3
	480	75.6	0.7	8.6	15.1
	580	19.3	0.5	33.1	47.1

According to TG, FTIR, and XPS results, the possible flame-retardant mechanism for LDPE/PA-APP$_7$ during the combustion is shown in Fig. 8, and it can be explained as follows. At the initial stage, the P—N—C structure was formed during the combustion process, which facilitated the formation of a stable char layer. Obviously, the formed char layer could protect part of LDPE from the decomposition. With increasing temperature, part of P—N—C, *etc*. structures decomposed under the catalytic effect of P—OH, accompanied by the formation of P—O—P, C=C, *etc*. structures and the release of H_2O and NH_3, which led to the formation of an intumescent, compact, and stable char layer, consequently the excellent flame-retardant performance of LDPE/PA-APP$_7$ was achieved.

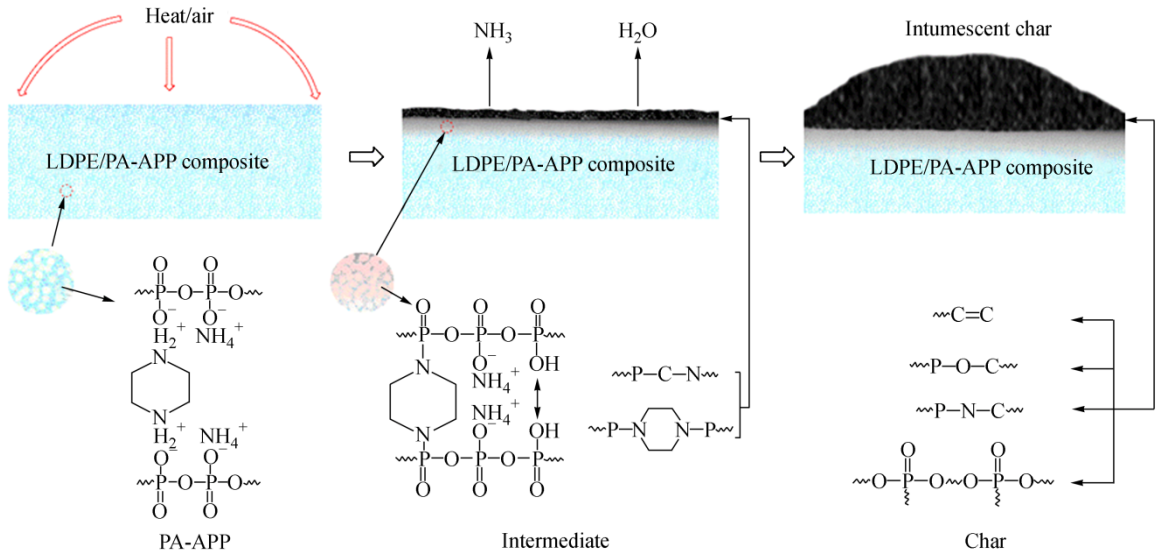

Fig. 8 Schematic diagram of possible flame-retardant mechanism for LDPE/PA-APP$_7$ during burning

CONCLUSIONS

In this work, PA-APP flame retardants with different structures were synthesized through ion exchange reaction. FTIR and ^{1}H-NMR tests confirmed that the PA-APP flame retardants were prepared successfully. Further, LOI and UL-94 tests demonstrated that PA-APP$_7$ was the most effective to flame retard LDPE among all these PA-APP flame retardants, which should be due to its good balance of the acid source, blowing source, and charring source. At the loading of 28 wt% PA-APP$_7$, flame-retarded LDPE could pass the UL-94 V-0 rating, and the LOI value reached 31.5%. Finally, TG, FTIR, and XPS tests were used to investigate the flame-retardant mechanism of PA-APP$_7$ with the balance of three sources. The formation of an intumescent char layer containing P—N—C, P—O—P, C=C, *etc*. structures, accompanied by the release of H_2O, NH_3, *etc*. gases, should be the most important reason for the good flame retardancy of LDPE/PA-APP$_7$ system.

REFERENCES

1 Abraham, D., George, K.E. and Joseph Francis, D., Eur. Polym. J., 1990, 26: 197
2 Ajji, A., Sammut, P. and Huneault, M.A., J. Appl. Polym. Sci., 2003, 88: 3070
3 Gao, H., Hu, S., Han, H. and Zhang, J., J. Appl. Polym. Sci., 2011, 122: 3263
4 Bourbigot, S. and Duquesne, S., J. Mater. Chem., 2007, 17: 2283
5 Hu, X.P., Li, W.Y. and Wang, Y.Z., J. Appl. Polym. Sci., 2004, 94: 1556
6 Xie, F., Wang, Y.Z., Yang, B. and Liu, Y., Macromol. Mater. Eng., 2006, 291: 247

7 Azizi, H., Barzin, J. and Morshedian, J., Express Polym. Lett., 2007, 1: 378
8 Bourbigot, S., Le Bras, M., Duquesne, S. and Rochery, M., Macromol. Mater. Eng., 2004, 289: 499
9 Hippi, U., Mattila, J., Korhonen, M. and Seppälä, J., Polymer, 2003, 44: 1193
10 Lu, K., Cao, X., Liang, Q., Wang, H., Cui, X. and Li, Y., Ind. Eng. Chem. Res., 2014, 53: 8784
11 Gao, Y., Wu, J., Wang, Q., Wilkie, C.A. and O'Hare, D., J. Mater. Chem. A., 2014, 2: 10996
12 Witkowski, A., Stec, A.A. and Hull, T.R., Polym. Degrad. Stab., 2012, 97: 2231
13 Shi, L., Li, D.Q., Wang, J.R., Li, S.F., Evans, D.G. and Duan, X., Clays Clay Miner., 2005, 53: 294
14 Braun, U., Schartel, B., Fichera, M.A. and Jaeger, C., Polym. Degrad. Stab., 2007, 92: 1528
15 Mueller, P., Fuhr, O. and Doering, M., Heteroat. Chem, 2013, 24: 252
16 Zhang, T., Yan, H., Shen, L., Fang, Z., Zhang, X., Wang, J. and Zhang, B., RSC Adv., 2014, 4: 48285
17 Huang, G., Yang, J., Wang, X., Gao, J. and Liang, H., J. Mater. Chem. A., 2013, 1: 1677
18 Molyneux, S., Stec, A.A. and Hull, T.R., Polym. Degrad. Stab., 2014, 106: 36
19 Rakotomalala, M., Wagner, S. and Doering, M., Mater., 2010, 3: 4300
20 Paul, K.T., Hull, T.R., Lebek, K. and Stec, A.A., Fire Saf. J., 2008, 43: 243
21 Wang, D., Liu, Y., Wang, D.Y., Zhao, C.X., Mou, Y.R. and Wang, Y.Z., Polym. Degrad. Stab., 2007, 92: 1555
22 Liu, X.Q., Wang, D.Y., Wang, X.L., Chen, L. and Wang, Y.Z., Polym. Degrad. Stab., 2011, 96: 771
23 Ciesielski, M., Schaefer, A. and Doering, M., Polym. Adv. Technol., 2008, 19: 507
24 Bourbigot, S., Le Bras, M., Dabrowski, F., Gilman, J.W. and Kashiwagi, T., Fire Mater., 2000, 24: 201
25 Tian, N., Wen, X., Jiang, Z., Gong, J., Wang, Y., Xue, J. and Tang, T., Ind. Eng. Chem. Res., 2013, 52: 10905
26 Li, B., Jia, H., Guan, L., Bing, B. and Dai, J., J. Appl. Polym. Sci., 2009, 114: 3626
27 Wang, B., Qian, X., Shi, Y., Yu, B., Hong, N., Song, L. and Hu, Y., Composites Part B, 2015, 69: 22
28 Nie, S., Zhang, M., Yuan, S., Dai, G., Hong, N., Song, L., Hu, Y. and Liu, X., J. Therm. Anal. Calorim., 2011, 109: 999
29 Camino, G., Costa, L. and Trossarelli, L., Polym. Degrad. Stab., 1985, 12: 203
30 Camino, G., Costa, L. and Luda di Cortemiglia, M.P., Polym. Degrad. Stab., 1991, 33: 131
31 Li, B. and Xu, M., Polym. Degrad. Stab., 2006, 91: 1380
32 Nie, S., Hu, Y., Song, L., He, Q., Yang, D. and Chen, H., Polym. Adv. Technol., 2008, 19: 1077
33 Shao, Z.B., Deng, C., Tan, Y., Chen, M.J., Chen, L. and Wang, Y.Z., ACS Appl. Mater. Interfaces, 2014, 6: 7363
34 Shao, Z.B., Deng, C., Tan, Y., Yu, L., Chen, M.J., Chen, L. and Wang, Y.Z., J. Mater. Chem. A., 2014, 2: 13955
35 Shao, Z.B., Deng, C., Tan, Y., Chen, M.J., Chen, L. and Wang, Y.Z., Polym. Degrad. Stab., 2014, 106: 88
36 Gottlieb, H.E., Kotlyar, V. and Nudelman, A., J. Org. Chem., 1997, 62: 7512
37 Wu, Z.P., Shu, W.Y. and Hu, Y.C., J. Appl. Polym. Sci., 2007, 103: 3667
38 Deng, C., Zhao, J., Deng, C.L., Lv, Q., Chen, L. and Wang, Y.Z., Polym. Degrad. Stab., 2014, 103: 1
39 Liu, G., Chen, W. and Yu, J., Ind. Eng. Chem. Res., 2010, 49: 12148
40 Camino, G., Costa, L. and Trossarelli, L., Polym. Degrad. Stab., 1985, 12: 213
41 Yan, Y.W., Chen, L., Jian, R.K., Kong, S. and Wang, Y.Z., Polym. Degrad. Stab., 2012, 97: 1423
42 Deng, C.L., Deng, C., Zhao, J., Li, R.M., Fang, W.H. and Wang, Y.Z., Chinese J. Polym. Sci., 2015, 33: 203